Raman Imaging with Near-field Scanning Optical Microscopy

C. L. Jahncke[(a)], M. A. Paesler, and H. D. Hallen

Department of Physics, North Carolina State University, Raleigh, NC 27695, USA

Raman spectroscopy in conjunction with near-field scanning optical microscopy is used to image Rb doped KTP within a spectral feature with high spatial resolution. We present Raman spectra as well as the first Raman images obtained in the near-field. Differences between near-field and far-field Raman measurements are discovered and discussed.

Spectral contrast adds an exciting dimension to near-field scanning optical microscope (NSOM) investigations. Among the first uses of wavelength discrimination in the near-field was the detection of fluorescence through subwavelength apertures[1]. Several years later, near-field signals were spatially and spectroscopically analyzed by studying the shift of the photoluminescence spectrum due to stresses in a Cr^{3+} ion implanted sapphire surface[2]. These spectra, however, were not taken while scanning. Recent work in near-field spectroscopy has included true spectroscopic imaging, i.e. near-field imaging undertaken within a spectral feature. For example, near-field luminescence has been used to investigate single quantum wells and quantum wires,[3] and the fluorescences of polystyrene spheres[4], biological cells[5] and of single molecules[6] have been examined. In this paper Raman scattering is added to the list of proven near-field spectroscopic imaging techniques.

Raman spectroscopy is a powerful tool for investigating a variety of materials. It is a nondestructive optical probe that provides chemical and physical information through the analysis of vibrational frequencies. Combined with the NSOM, Raman offers the possibility of determining chemical identity, material phase, stress, et cetera**,** with high spatial resolution. The gains in resolution, however, are not free. The price paid for high resolution is a considerably reduced signal. In addition, since the Raman effect has very low quantum efficiency (approximately 10^{-3} for liquids and as low as 10^{-6} for many solids), NSOM Raman experiments are difficult, but they can be done. A Raman spectrum obtained with a tapered fiber probe has been reported[7]. However, the probe was uncoated, which precludes high spatial resolution[8]. Furthermore, the tip to sample distance was merely estimated, and no imaging capabilities were demonstrated.

In order to gain the high spatial resolution provided by the NSOM, three things are required: 1) a subwavelength aperture, 2) the ability to position that aperture at a distance much less than the wavelength of the excitation light from a sample of interest -- i.e. in the sample's near-field, and 3) sufficient instrument stability to allow for imaging without destroying the desired resolution. In typical NSOM studies, long scan times are unnecessary and instrument drift poses little problem, but for Raman experiments, this is not the case. All three criteria have now been met in an NSOM possessing sufficient stability to allow for long scans
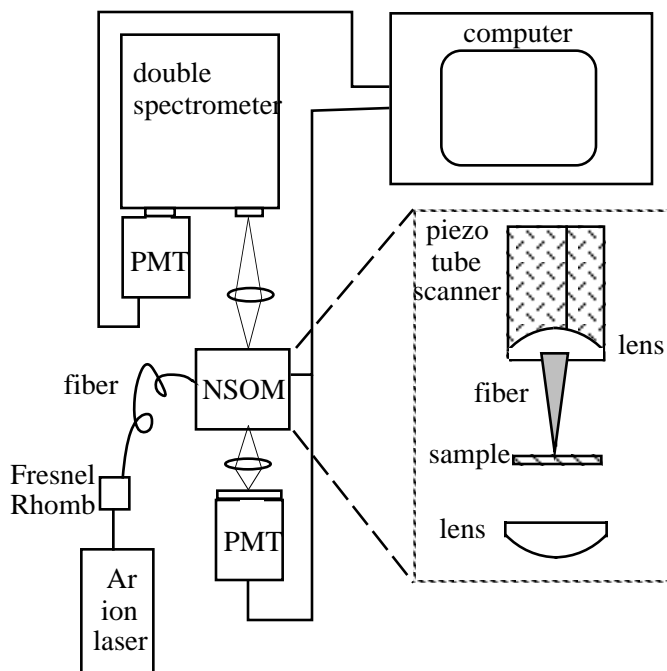

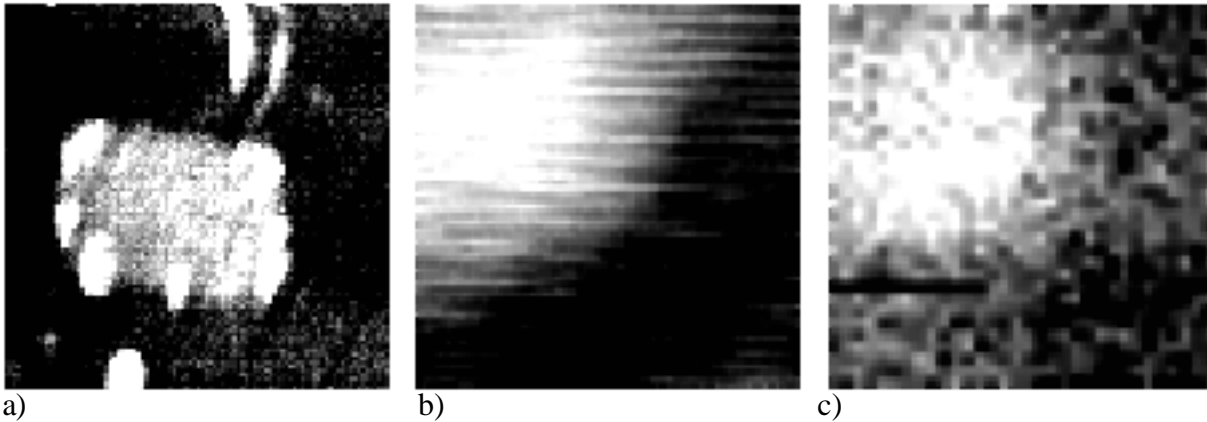Figure 1. Schematic of the experimental configuration.

a)   b)   c)

Figure 2.   Four images of a Rb doped KTP sample are shown.   a) is a 10 micron square topographic image, b) and c) are 4μm square images of the same corner of a Rb doped region. b) is a transmission image (the tailing around the square region is described in the text) and c) is a Raman image obtained in the near-field.

and thus true Raman spectroscopic imaging as demonstrated below.

Figure 1 is a schematic of the experimental setup. A cooled photomultiplier tube in the photon counting mode is used in conjunction with a SPEX Czerney-Turner double spectrometer for the Raman signal detection. An Argon Ion laser tuned to 514.5 nm provides the excitation source. The laser light is directed through an interference filter to remove plasma lines. A Fresnel Rhomb and/or waveplates rotate the polarization of the light before coupling it into the probe tip, which is mounted in the NSOM.

The NSOM uses conventional shear force feedback[9] to maintain a probe/sample separation of several nanometers.   The probes are fabricated by heating with a CO_2 laser, pulling and subsequently coating with aluminum to form a subwavelength aperture.   In this experiment, the sample is illuminated through the probe which is mounted into a 0.55 N.A. aspheric lens.   The backscattered light from the sample is collected with this lens and then focused into the spectrometer. The microscope provides for simultaneous collection of transmitted and reflected signals, therefore the transmitted light can be focused into a photomultiplier tube in order to perform simultaneous transmission studies. It is important to note that great care was taken in designing the microscope so that it would be stable[10], since low signal levels necessitate long integration times.

The material studied is potassium titanyl phosphate ($KTiOPO_4$ or KTP), a nonlinear optical material used for second harmonic generation. The sample contains an array of 5 micron square regions doped with rubidium through diffusion by potassium ion exchange, thus forming a rubidium titanyl phosphate (RTP) area. Doping results in a change in the refractive index, so that surface waveguides can be fabricated. A result of this process is a slight expansion of the KTP matrix which manifests itself in regions that are raised approximately 12 nm above the bulk KTP. Figure 2a shows a 10 micron square scan where the light area in the center is a typical Rb doped region. Figure 2b is a 4 μm square transmission image of a lower right hand corner of such a feature where contrast is observed since the Rb region has higher index of refraction by 0.027 than the KTP region. The long tails around the square region evident in the transmission image are probably due to the spreading of the optical field beneath the surface, where it encounters the 10 μm deep doped region.[11]

The Raman spectrum in the KTP region should differ from the RTP waveguide region due to the induced stress as well as the mass difference between K and Rb. Near-field Raman spectra from each region are shown in figure 3. The strongest feature in each spectrum is at 767 cm^{-1}. Ratios between this peak and other peaks in the spectra indicate that the 767 cm^{-1} peak is almost twice as high in the RTP region as in the bulk region.   While scanning the sample with the spectrometer tuned to this wavenumber, one would expect to see a higher Raman intensity in the
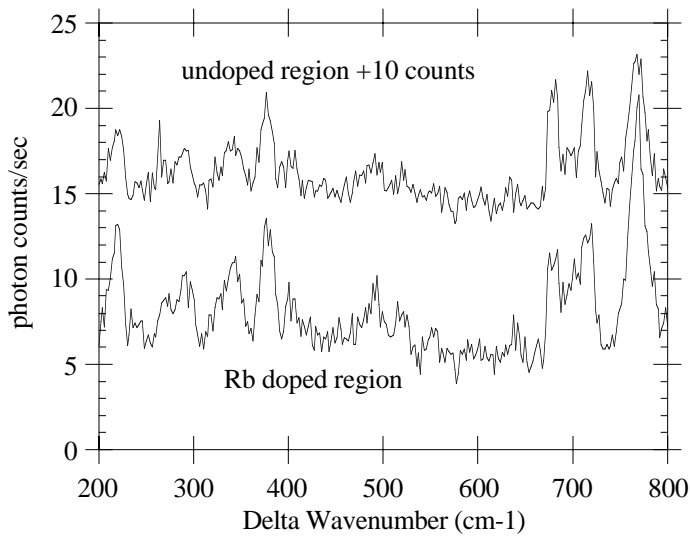
Figure 3. Two Raman spectra obtained in the near-field. The top spectrum is in the bulk KTP and the bottom spectrum is in the Rb doped region.

RTP regions. Figure 2c shows such a scan, where indeed the brighter region is coincident with the Rb doping. This 4µm square Raman image is of the same area as in figure 2b, and represents the first Raman image acquired in the near-field. The Raman image took over ten hours to complete. The sample drift during this time is ~3 Å/min corresponding to a ~200 nm drift over the *entire* duration of the scan. This compares well with the probe aperture size (which determines resolution), estimated to be ≈ 250 nm, which is similar to that used in other near-field spectroscopic studies[3]. The small Raman signal levels and consequent long integration times limit measurement possibilities. However, system improvements currently in progress should significantly improve the situation, making the technique more generally applicable.

In order to contrast the information obtained in the near-field with that in the far-field, a microRaman spectrum and a Raman spectrum taken through a fiber probe not in the near-field are shown in figure 4. The micro Raman spectrum is obtained in the same configuration as the nanoRaman. That is, the spectrometer and detection system are identical in the two experiments, and both of the signals are collected in a backscattering geometry. The microRaman experiment, however, involves the use of a 40x objective with a numerical aperture of 0.65 to illuminate the sample instead of the coated tapered fiber optic probe used in the nanoRaman case.

Two features should be highlighted in comparing the near-field vs. far-field spectra shown in figure 4. First, the Rayleigh tail in the spectrum obtained through the fiber optic probe is greatly reduced, if not eliminated over the spectral range shown in the figure. Since Rayleigh scattering is due to sample inhomogeneities, the reduction of this scattering observed through the probe illustrates that there is a smaller sampling volume in contrast with the microRaman case as expected. Raman scattering from the SiO_2 fiber is also vanishingly small in the near field case in figure 4. This would not be the case where the fiber is used to collect the Raman signal. Our preliminary results also suggest it would not be the case for an uncoated probe. Both the reduced Rayleigh scattering and lack of fiber background are important benefits in this low signal level experiment.

A second feature of particular interest is the spectral region around 700 cm^{-1}. Both the microRaman in figure 4a and the Raman data obtained with a probe in the far field
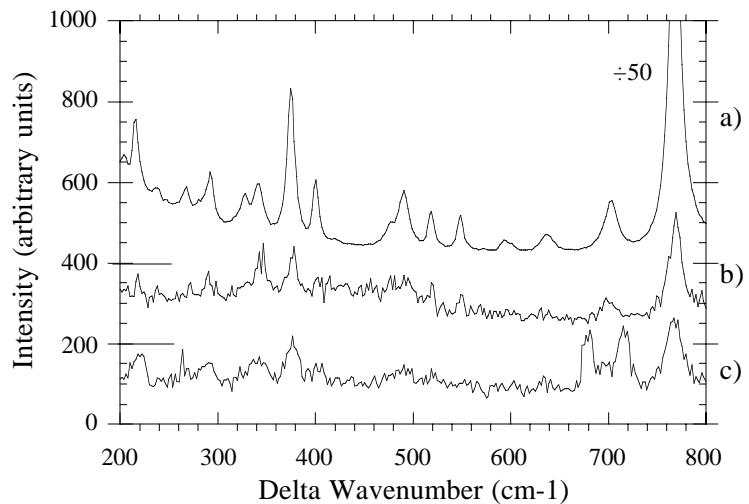

Figure 4. A comparison of Raman spectra in the near-field vs. the far-field. a) is a microRaman spectrum b) and c) are obtained through a fiber probe. b) is not in the near-field, and a) is in the near-field. The baseline levels of each scan are indicated by horizontal lines on the left of the graph.

in figure 4b show a single peak at 700 cm^{-1}. The near-field spectrum in figure 4c, on the other hand, has a doublet (or even arguably three peaks) centered around 700 cm^{-1}. There are several possible explanations for the different character of the near-field spectrum. The probe is expected to be more surface-sensitive than far-field techniques, since the metal coating on the probe can cause some surface enhancement[12]. Thus, the difference could reflect the change in the vibrational frequency due to nearby surface stress. Alternatively, the metal aperture and evanescent components can result in a z-polarization component which would not exist in the far field case[13]. This spectral region will be the focus of our future studies with nanoRaman on KTP.

In conclusion, we report the first Raman image obtained in the near-field. Background signals from the Rayleigh scattering and the fiber probe are very small over the spectral region studied. Evidence is given for surface sensitivity and surface enhancement of the Raman effect in the near-field experiments. All of these issues point to a promising future for near-field Raman studies.

References
(a)   Now at St. Lawrence University, Canton, NY 13617.
1   E. Betzig, A. Lewis, A. Harootunian, M. Isaacson, and E. Kratschmer, Biophys. J. **49**, 269 (1986).
        U. C. Fischer J. Opt.Soc. Am. **B3**, 1239 (1986).
2.   M. A. Paesler, P. J. Moyer, C. L. Jahncke, C. E. Johnson, R. C. Reddick, R. J. Warmack, and T. L. Ferrell, Phys. Rev. B. **42** 6750 (1990).
3.   R. D. Grober, T. D. Harris, J. K. Trautman, E. Betzig, W. Wegscheider, L. Pfeiffer, and K. West, Appl. Phys. Lett. **64**, 1421 (1994).
        H. F. Hess, E. Betzig, T. D. Harris, L. N. Pfeiffer, and K. W. West, Science **266**, 1740 (1994).
4.   J.K. Trautman, et. al., J. Appl. Phys. **71**, 4659 (1992).
5.   E. Betzig, R. J. Chichester, F. Lanni, and D. L. Taylor, Bioimaging 1994.
6.   J. K. Trautman, J. J. Macklin, L. E. Brus & E. Betzig, Nature **369**, 40 (1994).
        X. S. Xie and R. C. Dunn Science **265**, 361 (1994).
        W. P. Ambrose, P. M. goodwin, J. C. Martin, and R. A. Keller, Science **265**, 364 (1994).
        W. E. Moerner, T. Plakhotnik, T. Irngartinger, U. P. Wild, D. W. Pohl, and B. Hecht, Phys. Rev. Lett. **73**, 2764 (1994).
7.   D. P. Tsai, A. Othonos, M. Moskovits, and D. Uttamchandani, Appl. Phys. Lett. **64**, 1768 (1994).
8.   E. Buckland, P. J. Moyer, and M. A. Paesler, J. Appl. Phys. **73,** 1018 (1993).
        E. Betzig, T. D. Harris, J. S. Weiner, and R. L. Kostelak, Science **251**, 1468 (1991).
9.   E. Betzig, P. L. Finn, and J. S. Weiner, Appl. Phys. Lett **60**, 2484 (1992).
        R. Toledo-Crow, P. C. Yang, Y. Chen, and M. Vaez-Iravani, Appl. Phys. Lett. **60**, 2957, (1992).
10.   C. L. Jahncke and H. D. Hallen in preparation
11.   H. A. Bethe, Phys Rev. **66**, 163 (1994).
        E. Betzig, A. Harootunian, A. Lewis, and M. Isaacson, Applied Optics **25**, 1890 (1986).
12.   L. Novotny, D. W. Pohl, P. Regli, JOSA A **11**, 1768 (1994).
        D. A. Christenson Ultramicroscopy **57**, 189(1995).
13.   E. Betzig and R. J. Chichester, Science **262**, 1422 (1993).